SRTTU

Journal of Electrical and Computer Engineering Innovations

JECEI, Vol. 1, No. 2, 2013

Regular Paper

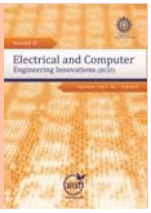

An Improved Time-Reversal-Based Target Localization for Through-Wall Microwave Imaging

A. B. Gorji[1,*] and B. Zakeri[1]

[1] Faculty of Electrical and Computer Engineering, Babol Noshirvani University of Technology, Babol, Iran

[*] Corresponding Author's Information: amin.gorji@stu.nit.ac.ir

ARTICLE INFO

ARTICLE HISTORY:

Received 27 October 2013
Revised 28 November2013
Accepted 4 December 2013

KEYWORDS:

Finite-difference time-domain
Optimum focusing
Target distance ratio
Target initial reflection
Through-wall microwave imaging
Time reversal

ABSTRACT

Recently, time reversal (TR) method, due to its high functionality in heterogeneous media has been widely employed in microwave imaging (MI) applications. One of the applications turning into a great interest is through-wall microwave imaging (TWMI). In this paper, TR method is applied to detect and localize a target obscured by a brick wall using a numerically generated data. Regarding this, it is shown that when the signals acquired by a set of receivers are time reversed and backpropagated to the target-embedded media, finding the optimum time frame which the constituted image represents a true location of the target becomes infeasible. Indeed, there are situations pertinent to the target distance ratio that the previously-used *Maximum field method* and *Entropy-based methods* may fail to select the optimum time frame. As a result, an improved method which is based on *initial reflection from the target* is proposed. According to different target locations described in this research, the results show this method prevails over the shortcomings of the former methods.

1. INTRODUCTION

Recently, in the field of microwave imaging (MI), the great interest on detection and localization of objects through walls and obstacles has been emerging. This phenomenon basically arises from various unique civilian and military applications, including non-destructive detection tests, earthquake search and rescue missions, hostage operations or hostile threat assessment situations [1]. In fact, a through-wall microwave imaging (TWMI) system would be capable of collecting information of the total media consisting of target(s) and wall(s), performing a comprehensive process on it, and also identify and localize the target. Encouraging results have been obtained with backscattering algorithms [2], synthetic-aperture-radar (SAR) [3], polarimetric-based techniques [4], tomographic approach [5], and high-speed imaging algorithm known as Envelope [6].

However, among the processing algorithms, time reversal (TR) methods have shown that would exploit ultra wide band (UWB) signals and the concept of multipath components in the intervening media to ameliorate the detection capabilities [7]. Originally, TR has been utilized in acoustics [8].Also, it has been introduced in Electromagnetics and more research has been carried out on subsurface object imaging [9], wireless communication systems [10], bio-malignant tissue detection [11, 12], and through-wall imaging of the obscured targets [13-15].

In TR method, a source radiates a signal which propagates through a media including the target. The waves are then reflected and the corresponding data are recorded by an array of receivers. By extracting the target-only responses from the data, reversing them in time and synthetically propagating them back, an image of the scene can be extracted at each time frame. Consequently, by utilizing an appropriate approach to take an optimum time frame, detection

and localization of the target becomes possible. Furthermore, in TWMI applications, TR entails to detect targets through materials including plywood, drywall, solid/hollow brick and concrete which their relative high permittivity or inhomogeneous structure may result in further burden for selecting the optimum time frame.

In this paper, we embark on solving the problem of finding an optimum time frame which represents an exact image of the target. In this regard, *Maximum Electric-field (E-field) Method* [13] and *Entropy-based Methods* [11, 14] have been recently employed in both TWMI and breast cancer detection scenarios. These methods may guarantee a maximum amplitude or a tightly focused image corresponding to the detected location of the target. However, we show that there are situations pertinent to the distance ratio of the target in which the preceding methods may fail to image the exact location of the target. As a result, an improved method, based on *initial reflection from the target* is proposed which is robust to the effect of this parameter and prevails over the previous methods.

The rest of the paper is organized as follows: in Section II a general description of TR method is presented. In Section III, the geometry of TWMI scenarios along with the specifications of computational setup is introduced which is carried out numerically using finite-difference time-domain (FDTD) [16]. In Section IV, the methods of finding an optimum time frame together with our proposed method are fully addressed. The results regarding the functionality of the methods to successfully localize the target according to different distance ratios of the target are demonstrated in Sections V. Finally, in Section VI a summary of the present work and the future contributions is drawn.

2. Classic TR Method

Time Reversal (TR) technique is an imaging method based on the invariance of Maxwell`s equations under time reversal, which is known in electromagnetics as the principle of reciprocity. In general, the procedure for detection and localization of the target based on TR consists of three main steps shown in Fig. 1.

After, a source radiates a signal through a media including the targets, the reflected waves from the media are recorded by an array of receiving antennas which ideally should be placed all around the media to capture all the possible directions of the reflected waves. However, unlike this full-aspect configuration [17], in other types of scenarios, it is presumably impossible to entirely surround the media and a limited number of arrays are particularly feasible.

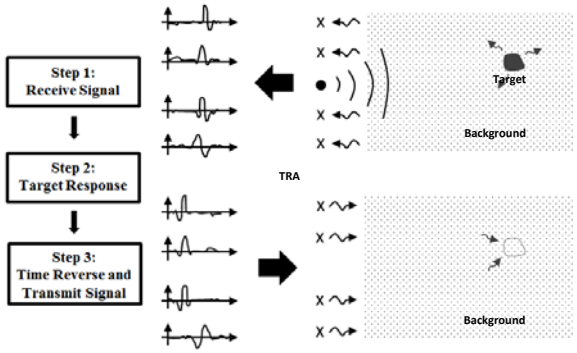

Figure 1: General scheme of TR method.

Then, the reflected waves from the media are recorded by an array of receiving antennas which ideally should be placed all around the media to capture all the possible directions of the reflected waves. However, unlike this full-aspect configuration [17], in other types of scenarios, it is presumably impossible to entirely surround the media and a limited number of arrays are particularly feasible. This limited-aspect configuration is in prevalent use for the applications including TWMI and subsurface objects imaging. Thereupon, the aim of forward propagation step is to collect the data of the media and process them in order to image and localize the targets. Accordingly, the data can be generated either analytically [7], numerically [11-13], or physically via on-site measurement [14], in which the first two suffices when one deals with the development of imaging algorithms such that spending time and energy on practical measurements is almost cumbersome.

Next, the target-only response must be extracted from the recorded signal at each array receiver. Since the recorded signal of the media consists of background clutter plus target, assuming that the background is stationary, its solo signature with no target in present can be calculated and collected at each receiver. Now, let`s assign E_T and E_B as the total and background reflected signals, respectively. Then, for each receiver, the target-only (scattered) response E_S is obtained as

$$E_S = E_T - E_B \tag{1}$$

This method of extracting the target response is called background subtraction method. In fact, extracting the target response is the basis of all TR processing methods including Classic TR [11], DORT [9, 18], MUSIC [19] and TRAIC [20]. In scenarios in which E_B cannot be obtained in a separate run, the target response is directly extracted from the total response by applying a time-window on the total signal [9] or Matched-Filter analysis [21]. However, these methods

will surely yield to more mathematical efforts. Additionally, in moving target scenarios, the information about E_B may not be required and corresponding target response can be achieved using the total response subtraction of two successive moving target runs. This method is called differential TR and is fully addressed in [22].

In the final step, based on TR processing method used in the previous step, imaging and localization of the target become possible. By time-reversing (phase conjugating in frequency domain) the target responses at each array receiver and synthetically propagating them back to the background media (no target), the wave focuses on the location of formerly existing target, approximately recreating the image of the target. It is obvious that this step is performed analytically by using Green functions named Point Spread Functions (PSF) [23] or numerically including FDTD [11-13], TLM [24], and Ray-Tracing methods [25]. Despite this, unlike the imaging applications, physical back propagation of the waves may occur in applications involving actual retransmission of signals like destruction of kidney stones with ultrasonic waves [26].

3. Geometry and Computational Setup

A. Geometry of TWMI Problem

The geometry of TWMI problem which is considered in this investigation is depicted in Fig 2. A standard commercial solid brick cell with dimensions 20×10 cm (length × width) is used here to construct a single layer wall with 10 cm thickness and 120 cm vertical length. Based on the measurement results reported in [27], the relative permittivity and conductivity of the brick wall is nearly consistent in the entire frequency spectrum of the measurement. As a result, regarding to the center frequency of excitation source, these values are set to ε_r=4.8 and σ=0.001 S/m.

A linear array of 16 isolated z-directed electric dipoles with equidistant separation of 6 cm are placed just 20 cm before the wall to act as the receiving probes. These arrays are called time reversal array (TRA) and will participate in synthetically back propagation step. The distance between the first and the last probe is called aperture size *a* which is equal to 90 cm for this array. A z-directed electric dipole atthe center of the array line is placed as the transmitter (and as monostatic receiver) to radiate the excitation pulse toward the scene in TM_z mode. Also, throughout this work, a cylindrical disk scattererwith diameter D=6 cm and ε_r=47 will be introduced as a target in different locations behind the wall, generally specified as near distance and far distance with respect to aperture size *a*. More discussion about this issue will be given in part D.

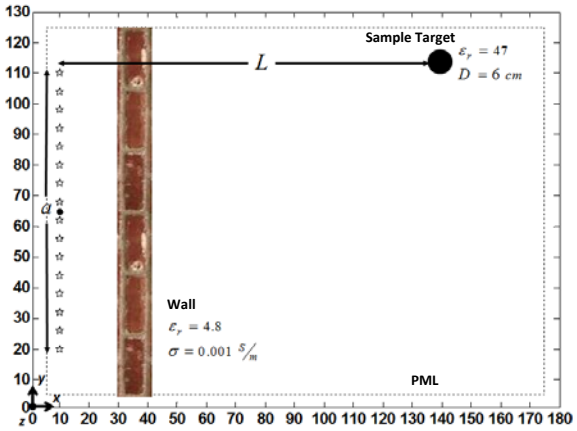

Figure 2: FDTD computational setup used for TWMI. The source (dot) and TRA (stars) are shown. The brick wall has 10 cm thickness. The target will be introduced at different locations. The aperture size and target distance are also denoted by *a* and *L*, respectively.

B. Computational Setup for TR Method

Both forward-propagation and back-propagation steps of TR method are carried out numerically using two-dimensional finite-difference-time-domain (FD-TD) method. The computational domain has a dimension of $N_x \times N_y$=180×130 grid points, with a uniform spatial discretization of Δ=1 cm and a time step of Δt=16 ps (the Courant factor S_c=c*Δt/Δx is chosen to be 0.5). The maximum of runtime is also set to maxtime=800Δt which is sufficiently enough for the incident wave to travel from the source to the right end of the domain in a round-trip. The boundary condition used is also a convolutional perfectly matched layer (CPML) formulated with recursive-convolution technique to provide reflectionless truncation of the computation domain. The thickness of CPML is set to 5Δ at all four sides of the boundaries.

It is also worth noting that in medium with high losses or dispersion, the performance of TR imaging based on conventional FDTD may become degraded due to double attenuation in forward and back propagation steps. To dispel this problem, a modification on FDTD update equations must be performed at back-propagation step in order to compensate losses or dispersion caused by the back-ground media [11, 28].

C. Excitation Source

In general, various constraints and specifications including particular electrical characteristics of the media, signal penetration through wall materials, target dimensions, and also portability of the setup will determine the best operating frequency range for microwave penetrating radar (MPR) systems. Practically, such systems operate in the range of 0.5-

10 GHz [29] and a minimum system bandwidth of about 30% with respect to the center frequency is essential for providing a sufficient resolution in target detection [4]. In this work, a UWB modulated Gaussian pulse is considered as the excitation source by

$$P(t) = e^{\left(\frac{t-t_s}{t_p}\right)^2} .\sin\left(2\pi f_p (t-t_s)\right) \quad (2)$$

Where t_p and t_s are temporal width and temporal shift, respectively, which specify the spectrum bandwidth of $P(t)$ and also f_p is the center frequency. These parameters are then assigned as f_p=4.6 GHz, t_p=0.16 ns and t_s=2*t_p. The excitation pulse and its frequency spectrum is also plotted in Fig. 3.

D. Final Settings

Assume that the target is located at a distance L away from the source. We may further investigate TR method according to the distance L with respect to a; simply L/a (originated from classical diffraction limit). As a result, there will be three distance ratios as near distance L/a<1, medium distance L/a=1, and far distance L/a>1. Finally, to fully understand the capability of TR method, two general near and far distance settings shown in Table 1 will be specified in this paper.

4. Focusing Methods

After exciting the source and collecting the data of reflected signals, we obtain target-only responses by using background subtraction methods. The target responses are then time reversed and backpropagated into the background media. Accordingly, the computationally backpropagated fields constitute an image of the scene at each frame of the time. Next, we embark on solving a problem of finding an *optimum timeframe* which represents an image of the scene with exact focusing on the location of the target.

A. Maximum E-field Method

As reported by Zheng et al. [13], in this method the maximum E-field amplitude of the imaging domain is found at each time frame and it is plotted along the time axis. The optimum time frame is then selected as a time which corresponds to the maximum of this plot, as

$$t_{opt}^{\text{Zheng}} = \left\{ t' : E_{\max}(t') > E_{\max}(t),\ t_0 < t < t_1 \ \ \& \ \ t \neq t' \right\} \quad (3)$$

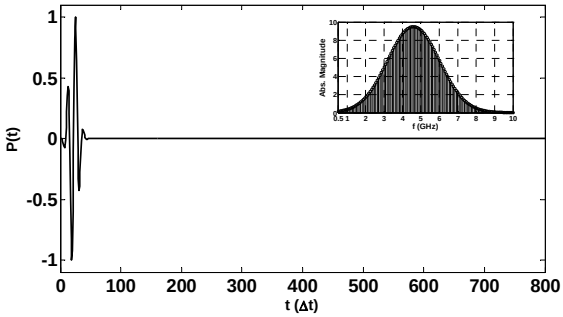

Figure 3: Modulated Gaussian excitation signal source and the corresponding frequency spectrum, f_p=4.6 GHz, t_p=0.16 ns, t_s=2*t_p.

TABLE 1
FINAL SETTINGS FOR TR PROCESSING

	Setting 1	Setting 2
Target Location (x,y)	(70,40)	(160,85)
Target Distance Ratio	near	far

B. Entropy-based Methods

In the ideal full-aspect configuration, the behavior of backpropagated waves on target location is such that it first converges toward the target and a time lag behind that, it diverges from it. In order to find a time frame which is corresponding to the convergence-divergence instant, a minimum entropy criterion will be defined as in (5) and (6) reported by Cresp et al [14] and Kosmas et al [11], respectively.

$$p_{ij}^n = \frac{E_n^{\,2}(i,j)}{\sum\sum_{i,j} E_n^{\,2}(i,j)} \quad (4)$$

$$ENT(n) = \frac{-\sum\sum_{\text{Cresp}} p_{ij}^n \ln p_{ij}^n}{\max(p_{ij}^n)} \quad (5)$$

$$ENT(n) = \frac{\left[\sum\sum_{\text{Kosmas}\ i,j} E_n^{\,2}(i,j)\right]^2}{\sum\sum_{i,j} E_n^{\,4}(i,j)} \quad (6)$$

Where n represents the time frame, (i,j) the grid cell coordinates and the summation is over the entire imaging domain. The defined entropy is calculated at each time frame and a time instant when it becomes minimized is selected as the optimum time frame. Unlike the previous method, minimum entropy method guarantees a tightly focused image rather than maximum field amplitude at the focusing point.

C. Target Initial reflection Method

In this work, we examine the functionality and efficiency of the above focusing methods and investigate the situations in which they may fail to image the exact location of the target. As a result, an alternative optimum time focusing method which is valid for all situations and prevails over the shortcomings of other methods should be utilized. In this part we are attempting to characterize this proposed method, namely *Target Initial Reflection Method*.

Let`s again postulate the geometry of the wall and an arbitrary located target as in Fig. 4. Now, we want to follow the transmitted wave starting at the beginning source point, propagating into the scene, possessing interactions with the wall and the target, and then reflecting back to the receiving arrays. In addition, we will monitor the target response waveforms of three particular receivers; the source receiver, which corresponds to a receiver at the source point (R_S), the nearest receiver to the target (R_N), and the farthest receiver away from the target (R_F). The excited source after a delay of t_d reaches to the peak value. In its path toward the target, it travels the route A_1B_1, B_1C_1 and C_1D, where D is the point which the transmitted wavefront is incident on the target. The target scatters the fields and a portion of them are received by the arrays. For the source receiver R_S, the scattered wave travels DC_1, C_1B_1 and B_1A_1, likewise the wave travels DC_2, C_2B_2 and B_2A_2 to reach to nearest receiver R_N, and DC_3, C_3B_3 and B_3A_3 to reach to farthest receiver R_F. The detailed waveforms monitored by each of these three receivers are shown in Fig. 5.

The received waves are then time-reversed and back-propagated, which is analogous to start the propagation from the right end of each waveform (maxtime) and move toward the left (Fig. 5). According to the depicted waveforms, the first antenna starting backpropagation process is the farthest one, it travels along the path toward the target up until the time the nearest antenna as the last antenna starts backpropagation. Based on Fig. 5 it is derived the two waveforms will simultaneously reach the target location D if they both travel only the remained time amount of t_2 which is the stacked time for the scattered waveform to travel from the target D to the nearest receiver at A_1. As a result, these two waveforms together with the waveform from the rest of the arrays will arrive at the same time to point D and their amplitudes are constructively added to each other to construct a contrasted image of the location of the target. More detailed route path of backpropagated waveforms are shown in Fig. 4.

In other words, the optimum time frame is a time instant in which the nearest receiver R_N is powered on

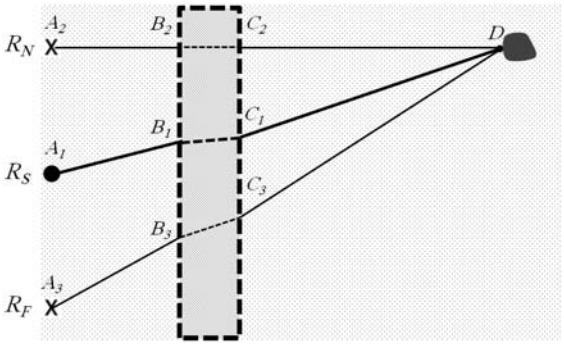

Figure 4: Detailed route path of forward and back propagated waveforms for source receiver (R_S), nearmost receiver (R_N), and farthest receiver (R_F).

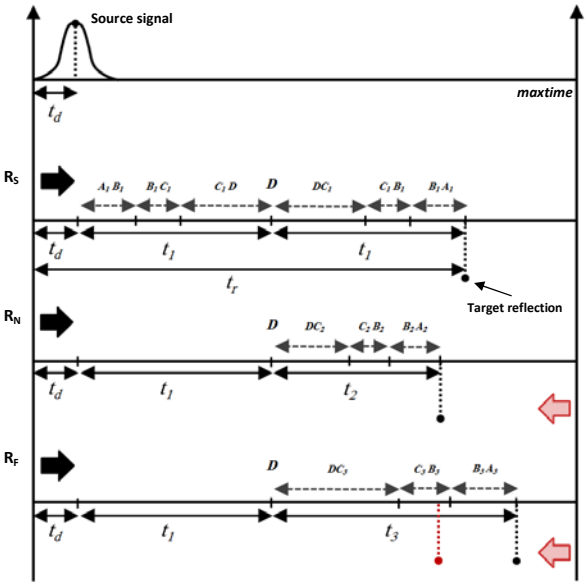

Figure 5: Signal waveforms monitored by each of source receiver (R_S), nearmost receiver (R_N), and farthest receiver (R_F). Time reversing and backpropagating the waveforms are analogous to start the propagation from the right end of the axis.

and then continues traveling for t_2 sec. To formulize the optimum time, we may write

$$t_{opt} = \underbrace{\left(maxtime\text{-}(t_d + t_1 + t_2)\right)}_{\text{R}_\text{N} \text{ is powered on}} + t_2 \qquad (7)$$

$$= maxtime - (t_d + t_1)$$

wheret_1 is the stacked time for the source waveform to travel from starting point A_1 to target D or vice versa. According to the waveform of the source receiver

$$t_r = t_d + 2t_1 \longrightarrow t_1 = \frac{t_r - t_d}{2} \qquad (8)$$

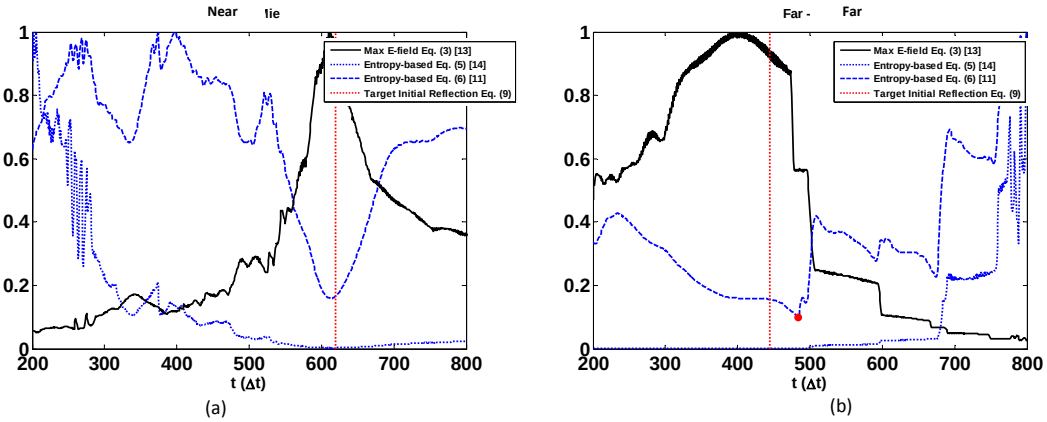

Figure 6: Curves of optimum time frame for *Maximum E-field Method*, *Entropy-based Methods Eq. (5) and Eq. (6)*, and *Target Initial Reflection Method*. (a) Near distance target (setting 1), (b) Far distance target (setting 2).

Where t_r is the time when the initial reflection from the target arrives to the source receiver.
As a result, by knowing the maxtime along with t_d and t_r, substituting (8) in (7), the optimum time frame t_{opt} could be readily derived as

$$t_{opt} = maxtime - \frac{t_r - t_d}{2} \tag{9}$$

The optimum time frame based on target initial reflection method guarantees well that the back-propagated waves of the entire receivers will simultaneously focus on a desired location which represents the target location. Here, further investigations prove that the analysis is independent of excitation sources and the wall parameters.

5. Localization of the Target

In this section, we investigates localization of a target for the settings defined in Section III and apply the focusing methods introduced in Section IV to select the optimum time frame for the target location.

Fig. 6 shows the corresponding curves for each of the focusing methods. Plots (a) and (b) also pertain to near and far distance ratios of the target. The optimum time frame derived by *Target Initial Reflection Method* is also determined by a vertical dashed line in each setting. All the curves are plotted from 200Δt which is an instant the backpropagated waves pass the wall, up to the maximum runtime of 800Δt. In order to compare the methods, the curves are normalized with respect to their corresponded maximum value. As it can be seen, plots of *Maximum E-field Method* have a monotonically increasing manner insofar as it reaches to the maximum and then starts to descend. Besides, in the case of multiple targets, additional local maxima are emerged instead of one global maximum.

TABLE 2
CALCULATED OPTIMUM TIME FRAME FOR EACH METHOD

	Setting 1	**Setting 2**
Max E-field	610 (9)	397 (48)
Entropy-based, Eq. (5)	614 (5)	405 (40)
Entropy-based, Eq. (6)	614 (5)	419 (26)
Target Initial Reflection	619	445

The *Entropy-based Methods* are monotonically decreasing up until their minimum value. Also noticeable is the small variation of *Entropy-based Method* (5) over almost the entire time axis. Furthermore for the cases the target is located at the right end of the imaging domain, as in setting 2 (Fig. 6b), *Entropy-based Method* (6) will have a global minimum (marked with red dot) which may be misled as the optimum time frame regarding the location of the target, whereas this minimum basically corresponds to the time instances the computationally backpropagated waves are exiting the imaging domain. Therefore the actual valid minimum is the one which is taking place at a time before reaching to this minimum. Finally, the optimum time frame concluded from the above curves for each method is depicted in Table 2. The difference (in terms of Δt) between each optimum time frame method with respect to *Target Initial Reflection Method* is also cited in parentheses.

Next, the images of spatial refocusing constituted by each method are demonstrated in Fig. 7 and Fig. 8 regarding near distance and far distance target location, respectively. The focused wave features a white region and the true location of the target is drawn as a small black circle. For near distance target (Fig. 7), it is clear from the images that the accurate focusing is almost achieved for all the methods including *Maximum E-field Method*, *Entropy-based Methods*, and *Target Initial Reflection Method*. On the other hand, when the target is located at far distance (Fig. 8), for all the methods (except *Target Initial*

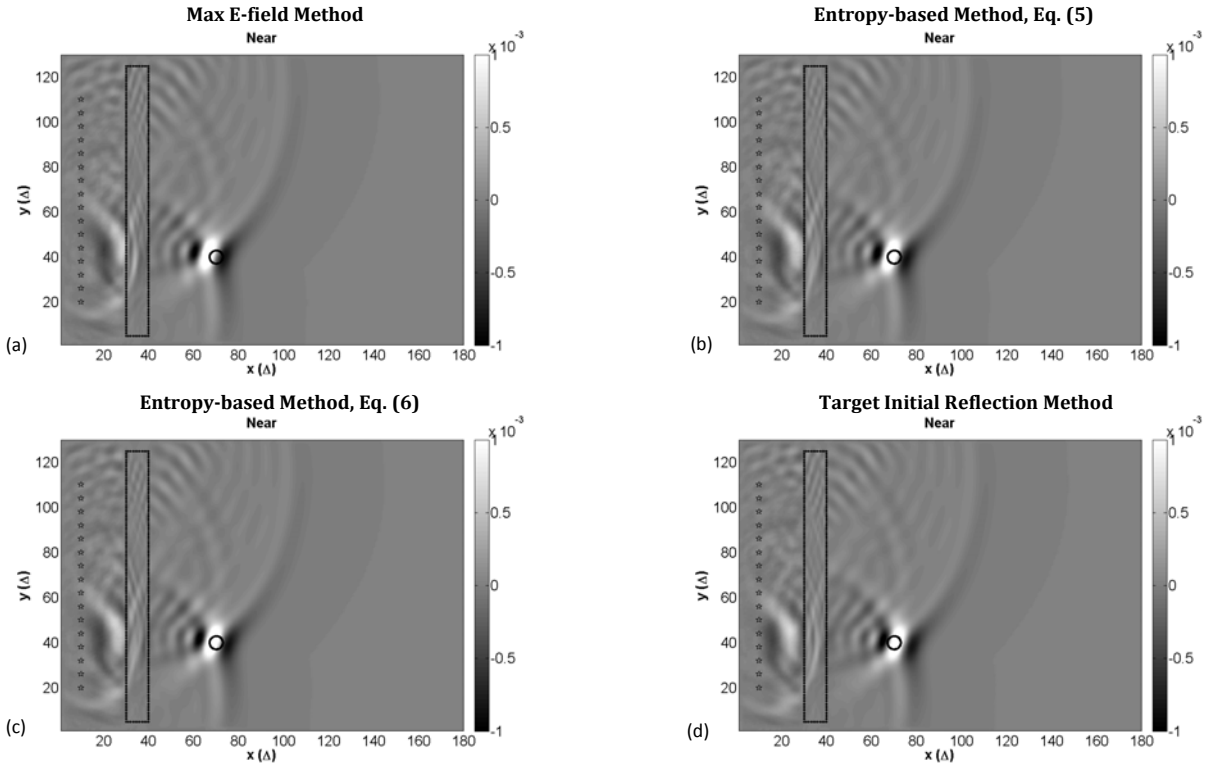

Figure 7: The images constituted by TR processing for target located at near distance (Setting 1) regarding optimum time frame methods of (a) *Maximum E-field Method*, (b) *Entropy-based Methods Eq.* (5),(c) *Entropy-based Methods Eq.* (6), (d) *Target Initial Reflection Method*.

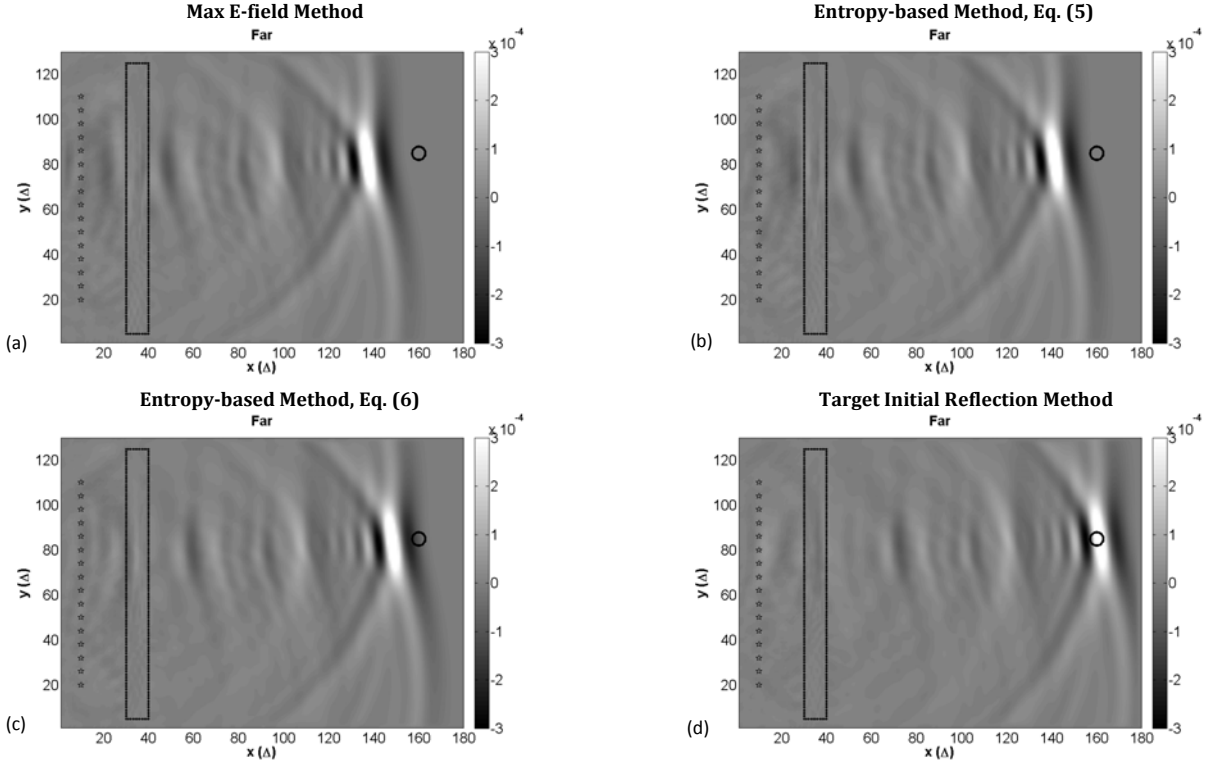

Figure 8: The images constituted by TR processing for target located at far distance (Setting 2) regarding optimum time frame methods of (a) *Maximum E-field Method*, (b) *Entropy-based Methods Eq.* (5),(c) *Entropy-based Methods Eq.* (6), (d) *Target Initial Reflection Method*.

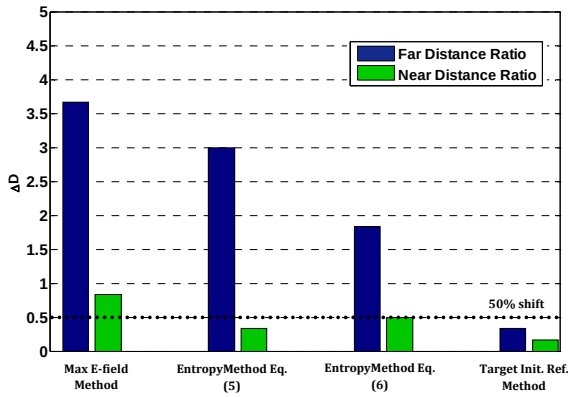

Figure 9: Difference between estimated and exact location of the target with respect to target distance ratios (far and near) for *Maximum E-field Method*, *Entropy-based Methods Eq.* (5) *and Eq.* (6), and *Target Initial Reflection Method*.

*Reflection Method) f*ocusing is achieved with considerable shift to the left from the exact target location which in fact may lead to an inaccurate judge about the existence of the target at its correct position. Also, noting that based on classic diffraction limit (*Focusing Width=λL/a*), the distance ratio increasing is the reason for decreasing the resolution of the focusing.

More quantitatively comparison of the images are depicted in Fig. 9 where for each method, the difference between the estimated location of the target and the exact location is calculated and represented on account of target diameter (size) D. For near distance target, all the *optimum time frame* methods estimate the target location with the accuracy of approximately less than one target size shift. In the case of far distance target, the only method which estimates the target as much near as the exact location is *Target Initial Reflection Method* with approximately less than half of the target size shift (50%). In general, we can conclude that *Entropy-based Methods* prevail over *Maximum E-field Method,* and *Target Initial Reflection Method* prevails over all of them without being totally dependent on the target near/far locations.

6. Conclusion

In this paper, TR method is employed to detect and localize a target behind a wall. In this research, the data were generated numerically using FDTD method for both forward and back propagation steps. In order to find the optimum time frame which represents an image of exact location of the target, *Maximum E-field Method*, *Entropy-based Methods*, and the proposed *Target Initial Reflection Method* were introduced. To evaluate the capability of these methods with respect to distance ratios (near and far) of the target, two general settings were specified. The results showed that when the target is located at near distances, accurate focusing was almost achieved for all the methods with the accuracy about less than one target size shift. However, for the far distance target, the only method which can estimate the target as much accurate as possible was *Target Initial Reflection Method* and all the other methods was failed to accurately focus on the target. In general, *Target Initial Reflection Method* prevailed over other methods without being totally dependent on the target different locations.

Future works may include:

1. Utilizing and evaluating this method in real TWMI scenarios where the nature of experimental environment would cause more deterioration for accurate localization of the target.
2. Applying this method for applications such as biological and under-the-ground imaging which their media are much heterogeneity.

7. References

[1] M. G. Amin and F. Ahmad, (2012, Sep., 27), Through-the-wall radar imaging: theory and applications, Villanova Univ., Villanova, PA.

[2] R. Zetik, S. Crabbe, J. Krajnak, P. Peyerl, J. Sachs, and R. Thoma, "Detection and localization of person behind obstacles using M-sequence through-the-wall radar," in *Proc. SPIE* , 2006, vol. 6201.

[3] M. Dehmollaian and K. Sarabandi, "Refocusing through building walls using synthetic aperture radar," *IEEE Trans. Geosci. Remote Sens.*, vol. 46, no. 6, pp. 1589-1599, Jun. 2008.

[4] K. M. Yemelyanov, N. Engheta, A. Hoorfar, and J. A. McVay, "Adaptive polarization contrast techniques for through-wall microwave imaging applications," *IEEE Trans. Geosci. Remote Sens.*, vol. 47, no. 5, pp. 1362-1374, May 2009.

[5] F. Soldovieri, R. Solimene, and G. Prisco, "A multiarray tomographic approach for through-wall imaging," *IEEE Trans. Geosci. Remote Sens.*, vol. 46, no. 4, pp. 1192-1199, Apr. 2008.

[6] S. Kidera, T. Sakamoto, and T. Sato, "High-resolution 3-D imaging algorithm with an envelope of modified spheres for UWB through-the-wall radars," *IEEE Trans. Antennas Propag.*, vol. 57, no. 11, pp. 3521-3529, Nov. 2009.

[7] A. Ishimaru, S. Jaruwatanadilok, and Y. Kuga, "Time reversal effects in random scattering media on superresolution, shower curtain effects, and backscattering enhancement." *Radio Sci.*, vol. 42, 2007.

[8] M. Fink, D. Cassereau, A. Derode, C. Prada, P. Roux, M. Tanter, J. Thomas, and F. Wu, "Time-reversed acoustics," *Rep. Prog. Phys.*, vol. 63, pp. 1933–1995, 2000.

[9] G. Micolau, M. Saillard, and P. Borderies, "DORT method as applied to ultrawideband signals for detection of buried objects," IEEE Trans. Geosci. Remote Sens., vol. 41, no. 8, pp. 1813-1820, Aug. 2003.

[10] H. T. Nguyen, J. B. Andersen, G. F. Pedersen, P. Kyritsi, and P. C. F. Eggers, "Time reversal in wireless communications: a measurement-based investigation," IEEE Trans. Wireless Commun., vol. 5, no. 8, pp. 2242-2252, Aug. 2006.

[11] P. Kosmas and C. M. Rappaport, "Time reversal with the FDTD method for microwave breast cancer detection," *IEEE Trans. Microw. Theory Techn.*, vol. 53, no. 7, pp. 2317-2323, Jul. 2005.

[12] Y. Chen, E. Gunawan, K. S. Loon, S. Wang, C. B. Soh, and T. C. Putti, "Time-reversal ultrawideband breast imaging: pulse design criteria considering multiple tumors with unknown tissue properties," *IEEE Trans. Antennas Propag.*, vol. 56, no. 9, pp. 3073-3077, Sep. 2008.

[13] W. Zheng, Z. Zhao, and Z. Nie, "Application of TRM in the UWB through wall radar," *PIER*,vol. 87, pp. 279-296, 2008.

[14] A. Cresp, I. Aliferis, M. J. Yedlin, Ch. Pichot, and J. Y. Dauvignac, "Investigation of time-reversal processing for surface-penetrating radar detection in a multiple-target configuration," in *Proc. 5th European Radar Conference*, Amsterdam, The Netherland, Oct. 2008.

[15] W. Zhang and A. Hoorfar, and L.Li, "Through-the-wall target localization with time reversal MUSIC method ," *PIER*, vol. 106, pp. 75-89, 2010.

[16] A. Taflove and S. C. Hagness, *Computational Electrodynamics: The Finite-Difference Time-Domain Method*, 3rd ed., Boston, MA: Artech House, 2005.

[17] J. P. Stang, "A 3D active microwave imaging system for breast cancer screening ," Ph.D. dissertation, Dept. Elec. Eng., Duke Univ., Durham, NC, 2008.

[18] M. Yavuz and F. L. Teixeira, "Full time-domain DORT for ultrawideband electromagnetic fields in dispersive, random inhomogeneous media," *IEEE Trans. Antennas Propag*., vol. 54, no. 8, pp. 2305-2315, Aug. 2006.

[19] A. J. Devaney, "Time reversal imaging of obscured targets from multistatic data," *IEEE Trans. Antennas Propag*., vol. 53, no. 5, pp. 1600-1610, May 2005.

[20] J. F. Moura and Y. Jin, "Time reversal imaging by adaptive interference canceling," *IEEE Trans. Signal Process.*, vol. 56, no. 1, pp. 233-247, Jan. 2006.

[21] P. Kosmas and C. M. Rappaport, "A matched-filter FDTD-based time reversal approach for microwave breast cancer detection," *IEEE Trans. Antennas Propag*., vol. 54, no. 4, pp. 1257-1264, Apr. 2006.

[22] N. Maaref, P. Millot, and X. Ferrieres, C.Pichot, and O. Picon, "Electromagnetic imaging method based on time reversal processing applied to through-the-wall target localization," *PIER*,vol. 1, pp. 59-67, 2008.

[23] D. Liu, J. Krolik, and L. Carin, "Electromagnetic target detection in uncertain media: time-reversal and minimum-variance algorithms," *IEEE Trans. Geosci. Remote Sens.*, vol. 45, no. 4, pp. 934-944, Apr. 2007.

[24] I. Scott, "Developments in time-reversal of electromagnetic fields using the transmission-line modeling method," Ph.D. dissertation, School of Elec. and Electron. Eng., Univ. of Nottingham, Nottingham, UK, 2009.

[25] D. Liu, G. Kang, L. Li, Y. Chen, S. Vasudevan, W. Joines, Q. H. Liu, J. Krolik, and L. Carin, "Electromagnetic time-reversal imaging of a target in a cluttered environment," *IEEE Trans. Antennas Propag*., vol. 53, no. 9, pp. 3058-3066, Sep. 2005.

[26] G. Montaldo, P. Roux, A. Derode, C. Negreira, and M. Fink, "Ultrasonic shock wave generator using 1-bit time-reversal in a dispersive medium: application to lithotripsy," Appl. Phys. Lett., vol.80, pp. 897–899, 2002.

[27] C. Thajudeen, A. Hoorfar, and F. Ahmad, "Measured complex permittivity of walls with different hydration levels and the effect on power estimation of TWRI target returns," *PIER*,vol. 30, pp. 177-199, 2011.

[28] M. Yavuz and F. L. Teixeira, "Frequency dispersion compensation in time reversal techniques for UWB electromagnetic waves," *IEEE Geosci. Remote Sens. Lett.*, vol. 2, no.2, pp. 233-237, Apr. 2005.

[29] J. D. Taylor, *Ultrawideband Radar: Applications and Design*, CRC Press, 2012.

BIOGRAPHIES

Amin B. Gorji was born in Cardiff, UK, in 1989. He received the B.Sc. degree in electrical engineering from Babol Noshirvani University of Technology, Babol, Iran, in 2011, where he is currently advancing his M.Sc. degree in Electromagnetics engineering.

Since 2010, he has been an assistant and researcher with the Antenna and Microwave Laboratory, Babol Noshirvani University of Technology.

His scientific fields of interest include microwave imaging based on time-reversal methods, time-domain channel modeling and wave propagation, and EM numerical techniques for solving scattering and radiation problems.

Bijan Zakeri was born in Babol, Iran, in 1974. He received the M.Sc. and Ph.D. degrees in Electromagnetics engineering from Amirkabir "Polytechnic" University of Technology, Tehran, Iran, in 1999 and 2007, respectively.

Since 2010, he is an Assistant Professor with Babol Noshirvani University of Technology, Babol, Iran. He is currently the head of Department of Communication and the director of Antenna and Microwave Laboratory at Babol Noshirvani University of Technology. He is also a member of Iranian Association of Information and Communication Technology.

His current research activities are in the fields of computational Electromagnetics, inverse scattering, radar microwave subsystems design, UWB antenna, and Polin-SAR remote sensing.